Magneto-electric point scattering theory for metamaterial scatterers

Ivana Sersic,* Christelle Tuambilangana, Tobias Kampfrath,† and A. Femius Koenderink

Center for Nanophotonics, FOM Institute for Atomic and Molecular Physics (AMOLF), Science Park 104, 1098 XG Amsterdam, The Netherlands

We present a new, fully analytical point scattering model which can be applied to arbitrary anisotropic magneto-electric dipole scatterers, including split ring resonators (SRRs), chiral and anisotropic plasmonic scatterers. We have taken proper account of reciprocity and radiation damping for electric and magnetic scatterers with any general polarizability tensor. Specifically, we show how reciprocity and energy balance puts constraints on the electrodynamic responses arbitrary scatterers can have to light. Our theory sheds new light on the magnitude of cross sections for scattering and extinction, and for instance on the emergence of structural chirality in the optical response of geometrically non-chiral scatterers like SRRs. We apply the model to SRRs and discuss how to extract individual components of the polarizability matrix and extinction cross sections. Finally, we show that our model describes well the extinction of stereo-dimers of split rings, while providing new insights in the underlying coupling mechanisms.

I. INTRODUCTION

Research in the field of metamaterials is driven by the possibility to control the properties of light on the nanoscale by using coupled resonant nanoscatterers to create optical materials with very unusual effective medium parameters. Engineering arbitrary values for the effective permittivity ϵ and permeability μ would allow new forms of light control based on achieving negative index materials[1–3], or transformation optics media[4] that arbitrarily reroute light through space. In order to reach such control over ϵ and μ, many metamaterial building nanoblocks have previously been identified as having an electric and magnetic response to incident light, including split ring resonators (SRRs)[5–10], rod-pairs[11], cut-wire pairs[12], fishnet structures[13–15] and coaxial waveguides[16]. In many instances, the nanoscatterers are not only interesting as building blocks in subwavelength lattices of designed ϵ and μ. The building blocks are in fact very strong scatterers with large cross sections[17–20], comparable to the large cross sections of plasmonic structures. Therefore, metamaterial building blocks are excellently suited to construct magnetic antennas, array waveguides and gratings in which electric and magnetic dipoles couple and form cooperative excitations, in analogy to the functionality imparted by plasmon hybridization[21]. Experiments outside the domain of effective media have appeared only recently. These experiments include experiments by Husnik *et al.*[17], and Banzer *et al.*[22] that quantify the extinction cross section of single split rings under differently polarized illumination, as well as a suite of experiments on coupled systems. These experiments include extinction measurements on split ring dimers[23] that point at resonance hybridization, as well as reports of magnetization waves[24], structural and geometrical chirality in arrays, as evident in e.g. massive circular dichroism[25–32], and chiral effects in split ring stereo-dimers studied by Liu *et al.*[33].

In order to understand the light-metamatter interaction in systems of strongly coupled magneto-electric scatterers, it is important to understand how individual metamaterial building blocks are excited and how they scatter. So far, explanations of the observed phenomena have mainly rested on two pillars. On the one hand, data are compared to brute force finite-difference time-domain (FDTD) simulations of Maxwell's equations, usually showing good correspondence[5,6,8,17,18,25,26]. While the FDTD method is a rigorous method, such numerical experiments do not in themselves provide insight into how split rings scatter or hybridize in coupled systems. There is general consensus that to lowest order, metamaterial interactions in lattices of scatterers like SRRs must be described by magneto-electric point-dipole interactions. Hence, simple LC circuit models with dipolar coupling terms are the second main interpretative tool to predict, e.g., frequency shifts due to electric and magnetic dipole-dipole interactions in lattices and oligomers[9,23,33,34]. To rationalize this LC circuit intuition, several authors have analyzed current distributions obtained by FDTD simulations in order to retrieve the microscopic parameters (*i.e.*, the polarizability) underlying such a dipolar interaction model, and in order to estimate multipolar corrections[18–20,35–38].

While there is general consensus that to lowest order, metamaterial interactions must essentially be magneto-electric point dipole interactions, we note that the dipolar circuit models in use so far have some significant shortcomings. Strictly speaking, the electric circuit theories lack the velocity of light c as a parameter. Hence, they contain no retardation or interference, they violate the optical theorem, do not predict quantitative cross sections, and fail to predict the effects of super- and subradiant damping on resonance linewidths. A fair comparison of intuitive point-dipole ideas with actual data is therefore impossible, unless a fully electrodynamic theory for magneto-electric point dipoles is derived. Such a theory would generalize the electric point scattering theory that is well known as very effective means to describe random media, extraordinary transmission and plasmon particle arrays[39–41]. In this paper we derive exactly such a theory for general magneto-electric scatterers. We show how reciprocity and energy conservation restrict the full magneto-electric response via Onsager constraints[42,43], and a new magneto-electric optical theorem for the full polarizability tensor. This tensor not only includes an electric (magnetic) response to electric (magnetic) driving, but also off-diagonal coupling in which a magnetic (electric) response results from electric (magnetic)

driving. While our theory sheds no light on the microscopic origin of the polarizability[44], we show how electrodynamic polarizability tensors can be directly constructed from LC circuit models. Furthermore we predict how extinction measurements and measurements of radiation patterns (i.e., differential scattering cross section) can be used to quantify the polarizability tensor.

The paper is structured in the following way: Firstly, in Section II we derive the general theory, taking into full account reciprocity, the optical theorem and radiation damping. In Section III we apply this theory to set up the polarizability of the archetypical metamaterial building block, a single SRR. In Section IV we show which set of experiments can be used to retrieve the tensor polarizability $\boldsymbol{\alpha}$. We find that magneto-electric coupling directly implies circular dichroism in the extinction of single split rings, evidencing the utility of our theory to describe structural chirality[25–32]. Thirdly, we show in Section V that the theory can be simply applied to obtain quantitative scattering spectra of coupled systems. By way of example we examine the case of two coupled resonators in the stereodimer configuration reported by Liu et al.[33].

II. MAGNETO-ELECTRIC POINT SCATTERER

A. Polarizability

A paradigm in scattering theory is the point dipole scatterer[39–41,45,46] to model scattering by very small, but strongly scattering particles. Generally, incident fields $\boldsymbol{E}$ and $\boldsymbol{H}$ induce a (complex) current distribution in an arbitrary scatterer. It is the express point of this paper to assess what the scattering properties are of subwavelength scatterers with strong electric and magnetic dipole moments, as this represents the physics expected of metamaterial building blocks[9,23,33,34,47]. Therefore we retain only electric and magnetic dipole terms, neglecting higher order multipoles. In such a theory, each scatterer is approximated as an electric dipole with an electric dipole moment $\boldsymbol{p} = \alpha_{EE}\boldsymbol{E}$ that is proportional to the driving electric field $\boldsymbol{E}$. The proportionality constant is the polarizability α_{EE}. In this paper, we derive a generalized point scattering theory for metamaterials that includes a magnetic dipole moment $\boldsymbol{m}$ on an equal footing with the electric dipole moment $\boldsymbol{p}$. In the most general case, the electric dipole moment $\boldsymbol{p}$ and magnetic dipole moments $\boldsymbol{m}$ are induced by both the external electric and magnetic fields $\boldsymbol{E}$ and $\boldsymbol{H}$ according to

$$\begin{pmatrix} \boldsymbol{p} \\ \boldsymbol{m} \end{pmatrix} = \boldsymbol{\alpha} \begin{pmatrix} \boldsymbol{E}_{\mathrm{in}} \\ \boldsymbol{H}_{\mathrm{in}} \end{pmatrix}. \tag{1}$$

Throughout this paper we suppress harmonic time dependence $e^{-i\omega t}$. We use a rationalized unit system that significantly simplifies all equations and is fully explained in Appendix A. In Eq. (1), $\boldsymbol{\alpha}$ is a 6×6 polarizability tensor, which consists of four 3×3 blocks, each of which describes part of the dipole response to the electric or magnetic component of the incident light

$$\boldsymbol{\alpha} = \begin{pmatrix} \boldsymbol{\alpha}_{EE} & \boldsymbol{\alpha}_{EH} \\ \boldsymbol{\alpha}_{HE} & \boldsymbol{\alpha}_{HH} \end{pmatrix}. \tag{2}$$

Here, $\boldsymbol{\alpha}_{EE}$ quantifies the electric dipole induced by an applied electric field. The tensorial nature of $\boldsymbol{\alpha}_{EE}$ is well appreciated in scattering theory for anisotropic particles, such as plasmonic ellipsoids[48]. By analogy with the electric response to electric driving quantified by $\boldsymbol{\alpha}_{EE}$, the tensor $\boldsymbol{\alpha}_{HH}$ quantifies the magnetic dipole induced by a driving magnetic field. Finally, the off-diagonal blocks represent magneto-electric coupling. The lower diagonal $\boldsymbol{\alpha}_{HE}$ quantifies the magnetic dipole induced by an incident electric field, and $\boldsymbol{\alpha}_{EH}$ quantifies the electric dipole induced by an incident magnetic field. Such magneto-electric coupling is well known to occur in the constitutive tensors of metamaterials[7]. Indeed, the first metamaterials consisted of split ring resonators, in which there is a magnetic response without any driving magnetic field in normal incidence experiments[49]. However, the relative strength of magneto-electric coupling in the polarizability, i.e., $\boldsymbol{\alpha}_{EH}$, and $\boldsymbol{\alpha}_{HE}$ have not been experimentally quantified.

B. Electrodynamic Onsager relation

There are several constraints on $\boldsymbol{\alpha}$. In addition to any symmetry of the scatterer itself that may impose zeros in the polarizability tensor, these constraints are due to reciprocity and to energy conservation. We start by examining the constraints imposed by reciprocity. It is well known from the field of bi-anisotropic materials[43] that reciprocity imposes so-called Onsager constraints on the most general constitutive tensors relating $(\boldsymbol{D}, \boldsymbol{B})$ to $(\boldsymbol{E}, \boldsymbol{H})$. Already García-García *et al.*[47] proposed that such Onsager constraints carry over directly to electrostatic polarizabilities. Here we rigorously derive Onsager relations for electrodynamic magneto-electric point scatterers. By, definition, the electric and magnetic fields due to the induced $\boldsymbol{p}$ and $\boldsymbol{m}$ are equal to

$$\begin{pmatrix} \boldsymbol{E}_{\mathrm{out}} \\ \boldsymbol{H}_{\mathrm{out}} \end{pmatrix} = \boldsymbol{G}^0(\boldsymbol{r}, \boldsymbol{r}') \begin{pmatrix} \boldsymbol{p} \\ \boldsymbol{m} \end{pmatrix}, \tag{3}$$

with a dyadic Green tensor $\boldsymbol{G}^0$ that describes the field at position $\boldsymbol{r} = (x, y, z)$ due to a dipole at $\boldsymbol{r'} = (x', y', z')$. The 6×6 Green dyadic of free space can be divided in four 3×3 blocks

$$\boldsymbol{G}^0(\boldsymbol{r}, \boldsymbol{r}') = \begin{pmatrix} \boldsymbol{G}^0_{EE}(\boldsymbol{r}, \boldsymbol{r}') & \boldsymbol{G}^0_{EH}(\boldsymbol{r}, \boldsymbol{r}') \\ \boldsymbol{G}^0_{HE}(\boldsymbol{r}, \boldsymbol{r}') & \boldsymbol{G}^0_{HH}(\boldsymbol{r}, \boldsymbol{r}') \end{pmatrix} \tag{4}$$

The 3×3 diagonals correspond to the familiar known electric field Green dyadic[40,41] and magnetic field Green dyadic of free space, which in our unit system (see Appendix) both equal

$$\boldsymbol{G}^0_{EE}(\boldsymbol{r}, \boldsymbol{r}') = \boldsymbol{G}^0_{HH}(\boldsymbol{r}, \boldsymbol{r}') = (\mathbb{I}k^2 + \nabla\nabla)\frac{e^{ik|\boldsymbol{r}-\boldsymbol{r}'|}}{|\boldsymbol{r}-\boldsymbol{r}'|}. \tag{5}$$

The off diagonal blocks correspond to the mixed dyadics that specify the electric field at $\boldsymbol{r}$ due to a magnetic dipole at $\boldsymbol{r'}$,

respectively the magnetic field at $\boldsymbol{r}$ due to an electric dipole at $\boldsymbol{r'}$. Explicitly:

$$\begin{aligned}\boldsymbol{G}^0_{EH}(\boldsymbol{r},\boldsymbol{r}') &= -\boldsymbol{G}^0_{HE}(\boldsymbol{r},\boldsymbol{r}') \\ &= ik\begin{pmatrix} 0 & \partial_z & -\partial_y \\ -\partial_z & 0 & \partial_x \\ \partial_y & -\partial_x & 0 \end{pmatrix}\frac{e^{ik|\boldsymbol{r}-\boldsymbol{r}'|}}{|\boldsymbol{r}-\boldsymbol{r}'|}.\end{aligned} \tag{6}$$

In this work we focus solely on scatterers made from reciprocal constituents, as is commonly true for the metallic scatterers that constitute metamaterials. Since the materials that compose our scatterers (typically gold and silver) satisfy reciprocity microscopically, the polarizability tensor must also lead to a scattering theory that satisfies reciprocity.

To derive reciprocity constraints on $\boldsymbol{\alpha}$, it is sufficient to examine the Green function in the presence of just one point scatterer at the origin. This Green function that quantifies the field at $\boldsymbol{r}_2$ due to a source at $\boldsymbol{r}_1$ in presence of a single scatterer at $\boldsymbol{r}_s$ can be written as[39,40,50]

$$\boldsymbol{G}(\boldsymbol{r}_1,\boldsymbol{r}_2) = \boldsymbol{G}^0(\boldsymbol{r}_1,\boldsymbol{r}_2) + \boldsymbol{G}^0(\boldsymbol{r}_2,\boldsymbol{r}_s)\boldsymbol{\alpha}\boldsymbol{G}^0(\boldsymbol{r}_s,\boldsymbol{r}_1), \tag{7}$$

Reciprocity requires for any Green function $\boldsymbol{G}$ (similarly split in four blocks) that

$$\begin{pmatrix} \boldsymbol{G}_{EE}(\boldsymbol{r}_2,\boldsymbol{r}_1) & \boldsymbol{G}_{EH}(\boldsymbol{r}_2,\boldsymbol{r}_1) \\ \boldsymbol{G}_{HE}(\boldsymbol{r}_2,\boldsymbol{r}_1) & \boldsymbol{G}_{HH}(\boldsymbol{r}_2,\boldsymbol{r}_1) \end{pmatrix} = \begin{pmatrix} \boldsymbol{G}_{EE}(\boldsymbol{r}_1,\boldsymbol{r}_2) & -\boldsymbol{G}_{EH}(\boldsymbol{r}_1,\boldsymbol{r}_2) \\ -\boldsymbol{G}_{HE}(\boldsymbol{r}_1,\boldsymbol{r}_2) & \boldsymbol{G}_{HH}(\boldsymbol{r}_1,\boldsymbol{r}_2) \end{pmatrix}^T \tag{8}$$

which is equivalent to noting that swapping source and detector leaves the detected field unchanged, up to a change in sign. Specifically, Lorentz reciprocity requires a transpose for the diagonal 3×3 blocks, meaning that swapping a detector and source of like character leaves the detected field unchanged. An extra minus occurs for the off-diagonal terms, *i.e.*, when swapping a magnetic (electric) detector with an electric (magnetic) source. It is easy to verify that Eq. (8) is indeed satisfied by the free space Green function $\boldsymbol{G}^0$.

Using this fact, we evaluate Eq. (8) for the Green function in Eq. (7) to find if reciprocity constrains $\boldsymbol{\alpha}$. Since reciprocity is clearly satisfied for the first term in Eq. (7), we now focus on the second term

$$\boldsymbol{G}^0(\boldsymbol{r}_2,\boldsymbol{r}_s)\boldsymbol{\alpha}\boldsymbol{G}^0(\boldsymbol{r}_s,\boldsymbol{r}_1) = \boldsymbol{G}^0(\boldsymbol{r}_1,\boldsymbol{r}_s)\boldsymbol{\alpha}\boldsymbol{G}^0(\boldsymbol{r}_s,\boldsymbol{r}_2). \tag{9}$$

Expanding the matrix products in Eq. (8) while making use of the reciprocity of the free Green function results in the Onsager relations for the dynamic polarizability:

$$\boldsymbol{\alpha}_{EE} = \boldsymbol{\alpha}^T_{EE}, \quad \boldsymbol{\alpha}_{HH} = \boldsymbol{\alpha}^T_{HH}, \quad \text{and} \quad \boldsymbol{\alpha}_{EH} = -\boldsymbol{\alpha}^T_{HE} \tag{10}$$

These relations are identical in form to the Onsager relations for constitutive tensors[43], but are now derived on very different grounds for the polarizability of electrodynamically consistent point scatterers. This gratifying result shows that the general point dipoles proposed in this work can be used as microscopic building blocks for an exact scattering theory that describes the formation of bi-anisotropic media from dense lattices of scatterers in the effective medium limit. Indeed, since the point scattering building blocks fulfill the Onsager constraints, they are natural building blocks to derive effective media constitutive tensors by homogenization that also satisfy the Onsager relations.

C. Optical theorem

It is well known in point scattering theory for electric dipoles that polarizability tensors are not solely limited by reciprocity and spatial symmetry, but also fundamentally by energy conservation. Indeed, energy conservation imposes an 'optical theorem' that constrains the polarizability of an electric dipole scatterer to ensure that (in absence of material absorption) extinction equals scattering[40]. We proceed to examine these constraints imposed on $\boldsymbol{\alpha}$. Let us first recapitulate the well known case of a scalar electric scatterer[39,40]. An electric scatterer will absorb and scatter part of the incoming light, that together make up the extinction of a dipole. Extinction for an electric scatterer corresponds to the work done by the incident field $\boldsymbol{E}$ in order to drive the dipole $\boldsymbol{p}$. The work per optical cycle needed to drive $\boldsymbol{p}$ equals $W = \ll \mathrm{Re}\boldsymbol{E}\cdot\mathrm{Re}\frac{d\boldsymbol{p}}{dt} \gg$, where $\ll\gg$ indicates cycle averaging. Evaluating the work per cycle, and dividing it by the incident intensity $I_{\mathrm{in}} = |\boldsymbol{E}|^2/2Z$ (Z the impedance of the host medium) leads to $\sigma_{\mathrm{ext}} = W/I_{\mathrm{in}} = 4\pi k\mathrm{Im}\alpha_{EE}$. Scattering corresponds to far field radiation radiated by the dipole $\boldsymbol{p}$. According to Larmor, the cycle-averaged scattered power is[51] $P = \frac{4\pi k^4}{3Z}|\boldsymbol{p}|^2$. Hence one obtains the well known cross sections

$$\sigma_{\mathrm{ext}} = 4\pi k\mathrm{Im}\alpha_{EE} \quad \text{and} \quad \sigma_{\mathrm{scatt}} = \frac{8\pi}{3}k^4|\alpha_{EE}|^2. \tag{11}$$

Equating extinction to scattering for nonabsorbing particles to impose energy conservation, gives rise to the optical theorem for the polarizability

$$\mathrm{Im}\alpha = \frac{2}{3}k^3|\alpha_{EE}|^2 \tag{12}$$

This equation for instance shows the well-known fact that a real (electrostatic) α_0, such as Rayleigh's polarizability $\alpha = 3V(\epsilon-1)/(\epsilon+2)$ for a small sphere of dielectric constant ϵ, never satisfies the optical theorem[52]. An electrostatic α_0 can be made to satisfy the optical theorem by adding radiation damping[40,41] to obtain the dynamic polarizability

$$\frac{1}{\alpha} = \frac{1}{\alpha_0} - i\frac{2}{3}k^3. \tag{13}$$

It is easy to verify that the albedo of a scatterer with polarizability given by Eq. (13) is

$$a = \frac{\sigma_{\mathrm{scat}}}{\sigma_{\mathrm{ext}}} = \frac{1}{1+\frac{2}{3}k^3\mathrm{Im}\alpha_0},$$

confirming that radiation damping indeed transforms any lossless electrostatic polarizability ($\mathrm{Im}\alpha_0 = 0$) into a scatterer that satisfies the optical theorem. Also material loss included in α_0 via ϵ evidently leads to a lossy scatterer $a < 1$, as expected. Many alternative derivations of Eq. (13) have appeared, for instance by making a size parameter expansion of dipolar Mie coefficients[53].

Inspired by the case of a simple electric dipole, we now generalize the optical theorem and the concept of radiation damping to the full 6x6 tensorial polarizability of arbitrary magneto-electric scatterers. In this case, the work done per unit cycle by the incident field $\boldsymbol{E}_{\mathrm{in}}$ and $\boldsymbol{H}_{\mathrm{in}}$ to drive $\boldsymbol{p}$ and $\boldsymbol{m}$ is equal to

$$W = \quad \ll \mathrm{Re}\boldsymbol{E}_{in} \cdot \mathrm{Re}\frac{d\boldsymbol{p}}{dt} + \mathrm{Re}\boldsymbol{H}_{in} \cdot \mathrm{Re}\frac{d\boldsymbol{m}}{dt} \gg \qquad (14)$$

which evaluates to

$$W = \frac{2\pi}{Z} k \mathrm{Im}\left[\begin{pmatrix} \boldsymbol{E}_{\mathrm{in}} & \boldsymbol{H}_{\mathrm{in}} \end{pmatrix}^* \boldsymbol{\alpha} \begin{pmatrix} \boldsymbol{E}_{\mathrm{in}} \\ \boldsymbol{H}_{\mathrm{in}} \end{pmatrix}\right], \qquad (15)$$

where $(\cdot)^*$ indicates complex conjugate. The power per solid angle radiated by the induced dipoles in a direction specified by a unit vector $\hat{\boldsymbol{r}}$ is easily found by calculating the far-field Poynting vector from Eq. (3). The result is composed of three terms:

$$\frac{dP}{d\Omega} = \frac{dP_p}{d\Omega} + \frac{dP_m}{d\Omega} + \frac{k^4}{2Z}\mathrm{Re}(\boldsymbol{p} \times \boldsymbol{m}) \cdot \hat{\boldsymbol{r}}, \qquad (16)$$

The first term in Eq. (16) represents the scattered radiation of just the electric dipole $\boldsymbol{p}$, which integrates to a total scattered power given by Larmor's formula. The second term in Eq. (16) represents the radiation pattern of just the magnetic dipole $\boldsymbol{m}$, again given by Larmor's formula. Note that both terms simply represent the well known $\sin^2\theta$ donut shaped radiation pattern for $\boldsymbol{p}$ and $\boldsymbol{m}$. The third term, however, can completely change the radiation pattern, as it contains the interference between the fields of $\boldsymbol{p}$ and $\boldsymbol{m}$. Hence the relative phase between the induced $\boldsymbol{p}$ and $\boldsymbol{m}$ is important for the differential scattering cross section. To obtain the total scattered power, one should integrate Eq. (16) over all solid angle. The interference term integrates to 0, as is easily seen from the fact it is an odd function of $\hat{\boldsymbol{r}}$. Therefore, Larmor's formula immediately generalizes, and the scattering cross section equals:

$$P = \frac{4\pi}{3Z} k^4 \left\| \begin{matrix} \boldsymbol{p} \\ \boldsymbol{m} \end{matrix} \right\|^2. \qquad (17)$$

Equating extinction to scattering results in a condition that must be satisfied for any incident field $(\boldsymbol{E}_{\mathrm{in}}, \boldsymbol{H}_{\mathrm{in}})$

$$\mathrm{Im}\left[\begin{pmatrix} \boldsymbol{E}_{\mathrm{in}} & \boldsymbol{H}_{\mathrm{in}} \end{pmatrix}^* \boldsymbol{\alpha} \begin{pmatrix} \boldsymbol{E}_{\mathrm{in}} \\ \boldsymbol{H}_{\mathrm{in}} \end{pmatrix}\right] = \frac{2}{3} k^3 \left[\begin{pmatrix} \boldsymbol{E}_{\mathrm{in}} & \boldsymbol{H}_{\mathrm{in}} \end{pmatrix}^* \boldsymbol{\alpha}^{*T} \boldsymbol{\alpha} \begin{pmatrix} \boldsymbol{E}_{\mathrm{in}} \\ \boldsymbol{H}_{\mathrm{in}} \end{pmatrix}\right], \qquad (18)$$

Due to the tensorial character of $\boldsymbol{\alpha}$ it is not immediately evident how to extract a useful optical theorem that constrains just the polarizability tensor $\boldsymbol{\alpha}$ without reference to any incident field $(\boldsymbol{E}_{\mathrm{in}}, \boldsymbol{H}_{\mathrm{in}})$. In order to eliminate $(\boldsymbol{E}_{\mathrm{in}}, \boldsymbol{H}_{\mathrm{in}})$ we make the assumption (verified below for split rings) that $\boldsymbol{\alpha}$ can be diagonalized. We call the eigenvectors $\boldsymbol{v}_i$, and denote the eigenvalues, which we will refer to as 'eigenpolarizabilities', with A_i. Expanding the incident field at the position of the origin in the orthogonal eigenvectors

$$\begin{pmatrix} \boldsymbol{E}_{\mathrm{in}} \\ \boldsymbol{H}_{\mathrm{in}} \end{pmatrix} = \sum_i c_i \boldsymbol{v}_i, \qquad (19)$$

and with $\boldsymbol{\alpha}\boldsymbol{v}_i = A_i \boldsymbol{v}_i$ and $\langle \boldsymbol{v}_i | \boldsymbol{v}_j \rangle = \delta_{ij}$, Eq. (18) reduces to

$$\frac{2}{3} k^3 \sum_{i=1}^{6} |c_i|^2 |A_i|^2 \geq \sum_{i=1}^{6} |c_i|^2 \mathrm{Im} A_i, \qquad (20)$$

with strict equality for lossless scatterers. Since this equation must be satisfied for any choice of incident wave (i.e., any combination of c_i), we find a generalized optical theorem for 6×6 polarizability tensors that can be expressed in terms of the eigenpolarizabilities as

$$\frac{2}{3} k^3 |A_i|^2 \geq \mathrm{Im} A_i \qquad \forall i = 1 \ldots 6, \qquad (21)$$

again with strict equality for lossless scatterers. Eq. (21) implies that the polarizability tensor represents an energy conserving scatterer, if and only if each of its 6 eigenpolarizabilities are chosen to satisfy the simple scalar optical theorem (Eq. (12)) derived for electric scatterers. This general optical theorem highlights the importance of two new quantities: the eigenpolarizabilities, and the corresponding eigenvectors of the point scatterer polarizability.

In Eq. (13) we reviewed the well-known addition of radiation damping required to make electrostatic polarizabilities satisfy the optical theorem. Since metamaterial scatterers are frequently treated via electrostatic circuit models, it would be extremely fruitful to generalize this method to general 6×6 electrostatic polarizability tensors. It is now evident, that we can simply apply the scalar recipe to each eigenpolarizability separately. An alternative notation for this method is:

$$\boldsymbol{\alpha}^{-1} = \boldsymbol{\alpha}_0^{-1} - \frac{2}{3} k^3 i \mathbb{I} \qquad (22)$$

We note that this expression, which is identical to Eq. (13) upon replacement of $1/(\cdot)$ by matrix inversion, provides a unique relation to translate a magneto-/electrostatic polarizability tensor $\boldsymbol{\alpha}_0$ derived from RLC circuit theory, to the corresponding electrodynamic polarizability that satisfies the optical theorem. We can hence consistently assess how intuitive ideas based on a microscopic RLC circuit model for electrostatic dipoles lead to quantitative predictions for extinction, scattering, as well as resonance hybridization, diffraction and super/sub radiant damping in coupled systems, such as periodic systems, or arbitrary finite clusters.

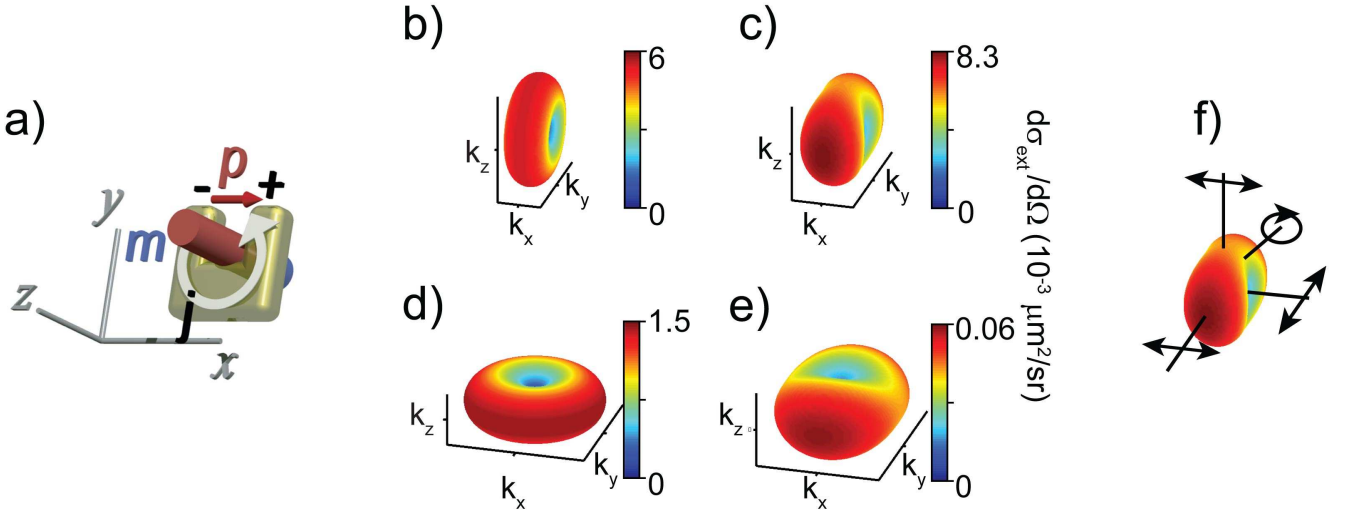

FIG. 1. Split ring radiation patterns corresponding to the polarizability tensor eigenvectors. Panel (a): (Sketch) A single split ring resonator can have an electric dipole moment $\boldsymbol{p}$ along the x-axis due to charging of the split. Circulating current j in the ring gives rise to a magnetic dipole moment $\boldsymbol{m}$ in the z-direction. Panels (b,c): Radiation patterns of the two eigenmodes of an SRR in the case of no off-diagonal magneto-electric coupling ($\eta_E = 0.7, \eta_H = 0.3, \eta_C = 0$). The electric dipole moment oriented along the x-axis radiates most of its amplitude in the ky, kz plane, while the magnetic dipole oriented along the z-axis radiates mostly into the kx, ky plane. Panels (d,e): radiation patterns of the eigenvectors with magneto-electric cross coupling ($\eta_C = 0.4$). Panel (f): indication of the polarization of the light radiated by the eigenvector with largest eigenvalue (panel (c)). Light is linearly polarized for wave vectors along the cartesian axes, but elliptically polarized in general. The direction of strongest circular dichroism in extinction and scattering is in the xz-plane.

III. POLARIZABILITY OF SPLIT RING RESONATORS

A. Symmetry

As an example of our general theory we consider the specific example of split ring resonators. The electrostatic polarizability of split ring resonators was discussed for instance by Garcìa-Garcìa et al[47]. We consider the LC resonance of an infinitely thin split ring in the xy plane, with split oriented along the x axis, as shown in Fig. 1(a). Incident electric field polarized along the x direction gives rise to an electric dipole $\boldsymbol{p} = (\alpha^{xx}_{EE} E_x, 0, 0)$ oriented along the split of the SRR. As in an LC circuit, the charge separation generated over the capacitive split relaxes as a circulating current, hence giving rise to a magnetic dipole $\boldsymbol{m} = (0, 0, \alpha^{zx}_{HE} E_x)$ in the z direction, in response to a driving E-field along x[54]. The same is valid vice versa: an applied magnetic field along z induces a magnetic dipole moment $\boldsymbol{m} = (0, 0, \alpha^{zz}_{HH} H_z)$ along the z direction. The associated current accumulates at the gap, giving rise to an electric dipole moment $\boldsymbol{p} = (\alpha^{xz}_{HE} H_z, 0, 0)$ driven by H_z. If we assume that the LC resonance really only involves $\boldsymbol{p}_x$ and $\boldsymbol{m}_z$, we find that the polarizability tensor is filled with zeros, except for the four contributions described above. Hence

$$\boldsymbol{\alpha}_{SRR} = \begin{pmatrix} \alpha^{xx}_{EE} & 0 & \dots & 0 & \alpha^{xz}_{EH} \\ 0 & & & & 0 \\ \vdots & & \ddots & & \vdots \\ 0 & & & & 0 \\ \alpha^{zx}_{HE} & 0 & \dots & 0 & \alpha^{zz}_{HH} \end{pmatrix}. \tag{23}$$

The symmetry constraints that set which elements of $\boldsymbol{\alpha}_{SRR}$ are zero, are valid both for the electrodynamic and electrostatic polarizability of split rings.

B. Quasi-electrostatic RLC model

We will now construct the electrodynamic polarizability by starting from an electrostatic polarizability derived from a single resonant RLC equation of motion. Therefore we take a common resonant frequency dependence out of the tensor elements, writing

$$\boldsymbol{\alpha}^{\text{static}}_{SRR} = \alpha(\omega) \begin{pmatrix} \eta_E & 0 & \dots & 0 & i\eta_C \\ 0 & & & & 0 \\ \vdots & & \ddots & & \vdots \\ 0 & & & & 0 \\ -i\eta_C & 0 & \dots & 0 & \eta_H \end{pmatrix}, \tag{24}$$

where η_E, η_C and η_H are constant and $\alpha(\omega)$ is a Lorentzian prefactor

$$\alpha(\omega) = \frac{\omega_0^2 V}{\omega_0^2 - \omega^2 - i\omega\gamma}. \tag{25}$$

Here, ω_0 is the SRR resonance frequency $\omega_0 \approx \frac{1}{\sqrt{LC}}$, γ is the damping rate due to the Ohmic loss of gold and V is the physical particle volume. As in the plasmonic case, this approximation is coined 'quasi-static', as it does contain frequency ω, but does not contain the velocity of light c. The polarizability obtained from the quasi-static polarizability once the radiation

damping term is added (section III C Eq. (22)) is called 'dynamic polarizability'. In this formulation, all the frequency dependence, and the units of $\boldsymbol{\alpha}_{SRR}$ are contained in $\alpha(\omega)$. The parameters η_E, η_H and η_C are dimensionless. For a lossless split ring η_E, η_H and η_C are all real. We assume that all losses are introduced via γ. To determine the sign of η_E, η_H and η_C, we expect that for very slow driving the charge (current) on the capacitor directly follows the driving E (H)-field, implying $\eta_E > 0$ and $\eta_H > 0$. The sign of η_C follows similar reasoning, After charge build-up, charge associated with a $\boldsymbol{p}_x = \mathrm{Re}(\alpha(\omega)\eta_E e^{-i\omega t}E_x)$ relaxes as counter-clockwise current, giving rise to a negative $\boldsymbol{m}_z = \mathrm{Re}(\alpha(\omega) i\eta_C e^{-i\omega t}E_x)$, implying that $\mathrm{sign}\,\eta_C = \mathrm{sign}\,\eta_E$.

C. Limit on magneto-electric coupling

Having constructed an electrostatic polarizability in accordance with RLC circuit models proposed in earlier reports, we apply radiation damping according to Eq. (22) to obtain a scatterer that has a correct energy balance:

$$\boldsymbol{\alpha}_{SRR}^{-1} = (\boldsymbol{\alpha}_{SRR}^{\mathrm{static}})^{-1} - \frac{2}{3}k^3\mathbb{I}. \tag{26}$$

So far we have not explicitly discussed absorption loss, except through the inclusion of the material damping constant γ in the quasi-static polarizability. Starting from a quasi-static polarizability with quasi-static eigenpolarizabilities A_i^{static}, the albedo for each eigenillumination $\boldsymbol{v}_i$ can be expressed as

$$a_i = \frac{1}{1 + \frac{2}{3}k^3 \mathrm{Im} A_i^{\mathrm{static}}}. \tag{27}$$

It follows that for any lossy scatterer the imaginary part of each eigenvalue A_i^{static} of the electrostatic polarizability tensor must be positive to ensure $0 \leq a \leq 1$. In the case of a tensorial $\boldsymbol{\alpha}$ with loss included as in Eq. (24), (25), one needs to explicitly verify that each eigenvalue has positive imaginary part. The eigenvalues of Eq. (24) are $A_{\pm}^{\mathrm{static}} = \alpha(\omega)\lambda_{\pm}$ with $\lambda_{\pm} = \frac{\eta_E + \eta_H \pm \sqrt{(\eta_E - \eta_H)^2 + 4\eta_C^2}}{2}$. Since $\mathrm{Im}(\alpha(\omega)) \geq 0$ and $\lambda_{\pm}$ are real, we find that both eigenvalues have positive imaginary part only if both λ_+ and λ_- are positive. Thus, loss sets an additional constraint on the polarizability tensor, and limits the magneto-electric coupling to

$$|\eta_C| \leq \sqrt{\eta_E \eta_H}. \tag{28}$$

This result implies a very important limitation on magneto-electric scatterers: it states that a magneto-electric cross coupling (η_C) can only be generated if there is a sufficiently strong directly electric, and directly magnetic response. We note that this constraint is very similar to the constraint on the magneto-electric cross coupling in constitutive tensors derived for homogeneous bi-anisotropic media in Ref. 43 that recently attracted attention in the framework of proposals for repulsive Casimir forces[55,56]. While our derivation was specific for split rings, we note that similar constraints hold for all magneto-electric scatterers. In the presence of material loss, the magneto-electric coupling terms are limited by the fact that all electrostatic eigenpolarizabilities must have positive imaginary part.

IV. PREDICTED SCATTERING PROPERTIES OF SINGLE SPLIT RINGS

In the remainder of the paper we discuss some insights that the proposed magneto-electric point scattering theory provides in how split rings scatter. In this section we will consider the eigenmodes and the radiation patterns of a single SRR for $\boldsymbol{\alpha}$ given by Eq. (26). Next, we predict which set of experiments will provide full information on the elements of the polarizability tensor. We will show how the extinction cross sections can be translated back to retrieve SRR polarizabilities and magneto-electric cross polarizabilities of a single SRR. Although the results we present are general, we use a specific set of parameters for all the figures presented in this paper. These parameters are chosen to fit to the properties of split rings that are resonant at $\lambda = 1.5\,\mu$m ($\omega_0/2\pi = 200$ THz and that consist of 200 by 200 nm gold split rings with a thickness of 30 nm and a gap width of 90 nm. Thus we take $V = 200 \times 200 \times 30$ nm^3. We set the damping rate to be that of gold $\gamma = 1.25 \cdot 10^{14}$ s^{-1} as fitted to optical constants tabulated in in Ref. 57. We use $\eta_E = 0.7$, $\eta_H = 0.3$ and $\eta_C = 0.4$. These parameters were chosen because (A) they reproduce quantitatively the extinction cross section under normal incidence along the z-axis measured by Husnik *et al.*[17], and (B) they fit well to our transmission data on arrays of different densities of split rings taken at normal incidence[9] and as a function of incidence angle[58]. The chosen values correspond to on-resonance polarizabilities $\alpha_{EE} = 4.6V$, $\alpha_{HH} = 2.1V$ and $\alpha_{EH} = 2.5V$, all well in excess of the physical SRR volume V as is typical for strong scatterers. Finally, we note that the calculated albedo fits well to the albedo $a = 0.5$ to 0.75 calculated by FDTD by Husnik et al.[17].

A. Radiation patterns and eigenvectors of the polarizability tensor

In Fig. 1, we consider the eigenstates of the split ring polarizability tensor presented in Eq. (26). We first assume that the cross coupling terms are absent, i.e., $\eta_C = 0$, in which case the polarizability tensor is diagonal, with eigenpolarizabilities $\alpha(\omega)\eta_E$ and $\alpha(\omega)\eta_H$. The corresponding orthogonal eigenmodes are $(p_x, m_z) = (1, 0)$ and $(p_x, m_z) = (0, 1)$. Figures 1 (b) and (c) show radiation patterns of the two eigenmodes. Figure 1(b) shows the radiation pattern of the purely electric eigenmode $(p_x, m_z) = (1, 0)$ and Fig. 1(c) shows the radiation pattern of the purely magnetic eigenmode $(p_x, m_z) = (0, 1)$. Note that both $\boldsymbol{p}_x$ and $\boldsymbol{m}_z$ radiate as simple dipoles with a $\sin^2\theta$ far field radiation pattern[51]. The two eigenmodes can be selectively excited by impinging with a plane wave incident along the z-axis with x-polarized E-field (electric eigenmode), or with a plane wave incident along the x-axis with y-polarization (z-polarized H-

field, magnetic eigenmode). The extinction cross section of a single split ring at these two incidence conditions is set by $\sigma_{\rm ext} = 4\pi k {\rm Im}(\alpha_{EE})$ and $\sigma_{\rm ext} = 4\pi k {\rm Im}(\alpha_{HH})$.

Next, we consider extinction and eigenmodes for arbitrary values of the cross coupling. It is easy to see that the extinction cross section at the two special illumination conditions (incident along z, x-polarized, respectively, incident along x, with y-polarization) remain equal to $\sigma_{ext} = 4\pi k {\rm Im}(\alpha_{EE})$ and $\sigma_{ext} = 4\pi k {\rm Im}(\alpha_{HH})$. However, for nonzero η_C, these incidence conditions and polarizabilities do not correspond anymore to the eigenvalues and eigenvectors of the polarizability tensor, which now have mixed magneto-electric character. In the extreme case of strongest magneto-electric coupling ($\eta_C = \sqrt{\eta_E \eta_H}$), the eigenvectors reduce to $(p_x, m_z) = (1, i\sqrt{\eta_E/\eta_H})$ and $(p_x, m_z) = (1, -i\sqrt{\eta_H/\eta_E})$. The associated far-field radiation patterns of these eigenvectors correspond to coherent superpositions of the radiation pattern of an x-oriented electric dipole, and a z-oriented magnetic dipole, with a quarter wave phase difference. Figures 1(d,e) show the on-resonance radiation pattern, assuming $\eta_E = 0.7$, $\eta_H = 0.3$ and η_C =0.4 . Note that these parameters are close to the limit of strongest possible magneto-electric coupling. Figures 1(d,e) reveal that the radiation pattern of each eigenmode is non-dipolar. Rather than a $\sin^2\theta$ donut-shaped pattern, an elongated radiation pattern occurs, with maximum extent in the y-direction. The polarization in the far field is linear for directions along the cartesian axis, but is generally elliptical.

B. Extinction cross sections to measure polarizability

Figure 2 shows the extinction cross section predicted by our point scattering model of a single split ring for different incidence conditions. In Fig. 2(a), the incident wave vector is swept from the z-direction to the y-direction, while maintaining $x-$ polarized light. For this set of incidence conditions the resulting extinction cross sections only depend on α_{EE} and α_{HH}, and are entirely independent of the off-diagonal coupling strength α_{EH}. The cross section increases from $\sigma_{\rm ext} = 4\pi k {\rm Im}\alpha_{EE}$ as the split ring is only driven by the incident E_x field when light is incident along z, to $\sigma_{\rm ext} = 4\pi k({\rm Im}\alpha_{EE} + {\rm Im}\alpha_{HH})$, as the split ring is driven by the incident E_x field plus the incident H_z field. When the wavevector is rotated to the the x-axis, the extinction cross section diminishes to $4\pi k {\rm Im}\alpha_{HH}$, as the split ring is only driven by H_z. The chosen values $\eta_E = 0.7, \eta_H = 0.3$ and $\eta_C = 0.4$ that we also used for Fig. 1(d,e) yield extinction cross sections $\sigma_{\rm ext} = 4\pi k {\rm Im}\alpha_{EE} = 0.29\ \mu{\rm m}^2$ and $\sigma_{\rm ext} = 4\pi k {\rm Im}\alpha_{HH} = 0.13\ \mu{\rm m}^2$. The predicted $\sigma_{\rm ext} = 4\pi k {\rm Im}\alpha_{EE} = 0.29\ \mu{\rm m}^2$ is consistent with the measurement ($\sigma_{\rm ext} = 0.3\ \mu{\rm m}^2$) reported by Husnik et al.[17]. It is important to note that measurements along cartesian incidence directions and with linear cartesian polarizations yield only the diagonal elements of the polarizability tensor. Indeed, the proposed measurements form a redundant set of measurements of α_{EE}, α_{HH}, and $(\alpha_{EE}+\alpha_{HH})$, but do not provide any insight into the magneto-electric cross coupling in the electrodynamic polarizability tensor.[59]

In order to measure the eigenpolarizabilities, it is necessary to selectively address the eigenvectors of the polarizability tensor. As noted above, the eigenvectors in the case of strong magneto-electric coupling $\eta_C \approx \sqrt{\eta_E \eta_H}$ tend to $(p_x, m_z) = (1, i\sqrt{\eta_E/\eta_H})$ and $(1, -i\sqrt{\eta_H/\eta_E})$. These eigenvectors require simultaneous driving by E_x and H_z, with a quarter wave phase difference. We note that such fields can be generated by circularly polarized light with incident wave vector constrained to the xz-plane. Indeed, at maximally strong magneto-electric coupling and $\eta_E = \eta_H$, circularly polarized light incident at 45° from the z-axis would selectively excite exactly one eigenmode. Therefore, we expect angle-resolved extinction measurements for oppositely handed circularly polarized beams to reveal the eigenpolarizabilities. Figure 2(b) plots the extinction cross section for right handed circular polarization, as a function of angle of incidence in the z-plane, for illumination tuned to the LC resonance frequency. Naturally, at normal incidence the extinction is exactly half the extinction obtained for linear polarization, as a consequence of the fact that E_y does not interact with the split ring at all. Strikingly, the extinction cross section is predicted to behave asymmetrically as a function of incidence angle. The extinction increases when going to positive angle and decreases when going to negative angle. Changing handedness is equivalent to swapping positive and negative angles. A detailed analysis shows that the maximum in extinction corresponds to the largest eigenvalue of the polarizability tensor ($\sigma_{ext} = 2\pi k {\rm Im}\alpha_+$), while the minimum in extinction corresponds to the smallest eigenvalue ($\sigma_{ext} = 2\pi k {\rm Im}\alpha_-$). Therefore, circularly polarized measurements reveal the eigenvalues of the polarizability tensor. Combining such circularly polarized extinction measurements with the measurements under cartesian incidence in Fig. 2(a), therefore allows to extract all components of the polarizability tensor. In addition to the contrast in extinction, the angle at which the maximum circular dichroism occurs is a second, independent measure for the magneto-electric coupling strength. The measurements in Fig. 2(a) and (b) together hence provide full, even redundant, information on η_E, η_H and η_C.

C. Structural chirality

The results plotted in Fig. 2(b) show that magneto-electric coupling in the 6×6 polarizability tensor directly implies structural chirality. It is exhilarating that this interesting phenomenon first reported by[26,30] for the transmission of arrays of scatterers is naturally present in the theory. However, while previous analysis of structural chirality focused on transmission through periodic arrays, we predict that circular dichroism already appears in the extinction cross section of a single split ring, with a strength set by how close the magneto-electric coupling strength is to its limit $\sqrt{\eta_E, \eta_H}$. The circular dichroism in extinction occurs independently of whether there is material loss, as opposed to, e.g., asymmetric transmission phenomena through arrays, that are claimed to require dissipation[30]. For maximally magneto-electrically coupled systems, the smallest eigenvalue is identically zero, implying that such

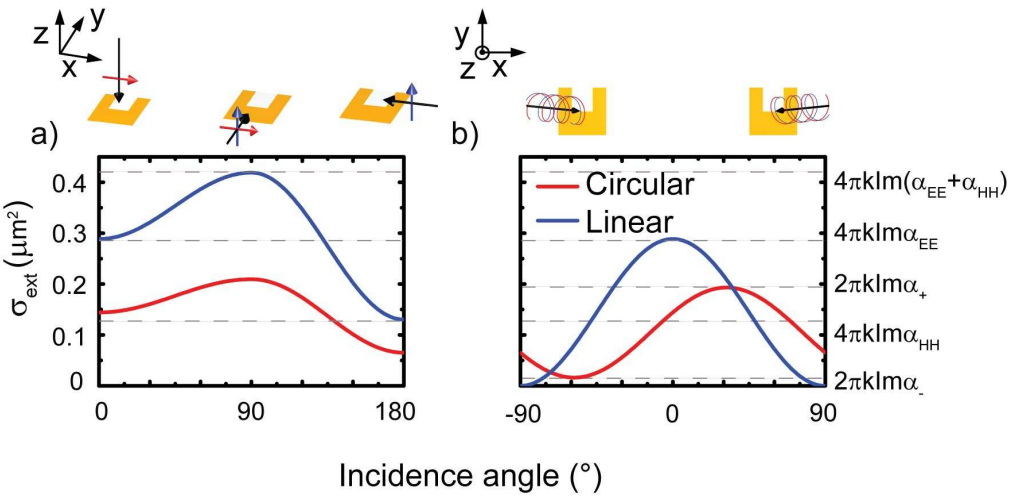

FIG. 2. Extinction cross section σ_{ext} as a function of the illumination angle and polarization. Blue lines represent σ_{ext} for linearly polarized incident illumination, while red lines represent extinction for right handed circularly polarized illumination. Panel (a) shows extinction for incidence wave vectors ranging from k_z to k_y to k_x. At normal incidence with k along the z-axis, σ_{ext} is a measure for only α_{EE} as E_x is the only driving field. Increasing the angle to 90° both polarizations E_x and H_z excite the dipoles in the SRR, so σ_{ext} is a measure for the sum of the terms on the diagonal of the polarizability tensor $(\alpha_{EE} + \alpha_{HH})$. Changing the angle to couple only the H_z of the incident light to the SRR gives σ_{ext} that is a measure for purely α_{HH}. Panel (b) σ_{ext} as a function of the incident angle in the xz-plane (wave vector ranging from $-k_x$ to k_z to k_x). For right-handed circular polarization minima and maxima in σ_{ext} occur as a function of angle, which are a measure for the eigenpolarizabilities α_- and α_+, respectively. Both sets of measurements in panel (a) and (b) together provide information on all the components of the polarizability tensor, α_{EE}, α_{HH}, and α_{EH}.

a scatterer is transparent for one circular polarization, and achieves its strongest scattering for the opposite handedness. We expect that our 6×6 polarizability tensor can be successfully used to describe all structurally chiral scatterers reported today, as well as clusters and periodic arrays thereof.

V. A COUPLED SYSTEM: SPLIT RING DIMERS

So far, this manuscript has focused purely on the scattering properties of single magneto-electric point scatterers. In the remainder of the paper we illustrate that our method can be easily used to analyze multiple scattering by magneto-electric scattering clusters. In order to calculate the response of a system of coupled magneto-electric dipoles, we generalize the general self-consistent equation that describes scattering of clusters of electric dipoles $\boldsymbol{p}$ as reviewed in[41]. Assuming a system of N magneto-electric point scatterers situated at positions $\boldsymbol{r}_1 \ldots \boldsymbol{r}_N$, the response upon illumination by an incident field $(\boldsymbol{E}_{\rm in}(\mathbf{r}), \boldsymbol{H}_{\rm in}(\mathbf{r}))$ is determined by a set of N self consistent equations for the induced dipole moments in each scatterer. The dipole moment induced in scatterer n with polarizability tensor $\boldsymbol{\alpha}_n$ is

$$\begin{pmatrix} \boldsymbol{p}_n \\ \boldsymbol{m}_n \end{pmatrix} = \boldsymbol{\alpha}_n \left[\begin{pmatrix} \boldsymbol{E}_{\rm in}(\mathbf{r}_n) \\ \boldsymbol{H}_{\rm in}(\mathbf{r}_n) \end{pmatrix} + \sum_{\substack{q=1\ldots N \\ q\neq n}} \boldsymbol{G}^0(\boldsymbol{r}_n, \boldsymbol{r}_q) \begin{pmatrix} \boldsymbol{p}_q \\ \boldsymbol{m}_q \end{pmatrix} \right] \tag{29}$$

Using this equation we can attempt to reinterpret recent measurements that evidence significant coupling in split rings in 2D arrays, as well as in oligomers[9,23,33,34]. Here we focus on the extinction of a dimer of split rings in socalled 'stereodimer'configuration, first studied by Liu et al.[33]. Figure 3 shows such a 'stereodimer', consisting of two SRRs in vacuum ($V = 200 \times 200 \times 30$ nm^3, resonant at a wavelength around 1500 nm), both parallel to the xy plane, vertically stacked with a small height difference of 150 nm. The upper SRR is rotated by a twist angle ψ around the z-axis. On the basis of the report by Liu et al.[33], we expect two resonance peaks with an angle dependent splitting, which can be explained in an LC model as the summed effect of electric dipole-dipole coupling and magnetic dipole-dipole coupling.

We calculate the extinction versus twist angle and wavelength of an incident beam incident from the $+z$ direction, with x-polarization. This beam directly excites $\boldsymbol{p}_x$ in both rings, which also drive each other. We first analyze the experiment assuming that there is no magneto-electric coupling term (setting η_C =0, although we keep η_E =0.7 and η_H = 0.3). As Fig. 3(b) shows, the extinction shows a single strong resonance that is blueshifted relative to the single SRR resonance at 200 THz. As a function of twist angle, this broad resonance redshifts to 200 THz at a twist of 90°, and shifts back to 220 THz at a twist of 180°. There is no sign of a second resonance, which might be hidden below the strong resonance. To bring out the second resonance more clearly, we reduce the loss in Fig. 3(b), to a 10 times lower value $\gamma = 1.25 \cdot 10^{13}$ s^{-1}) for gold in Fig. (c) and (d). For this almost absorption-free system, Fig. 3(c) indeed shows two

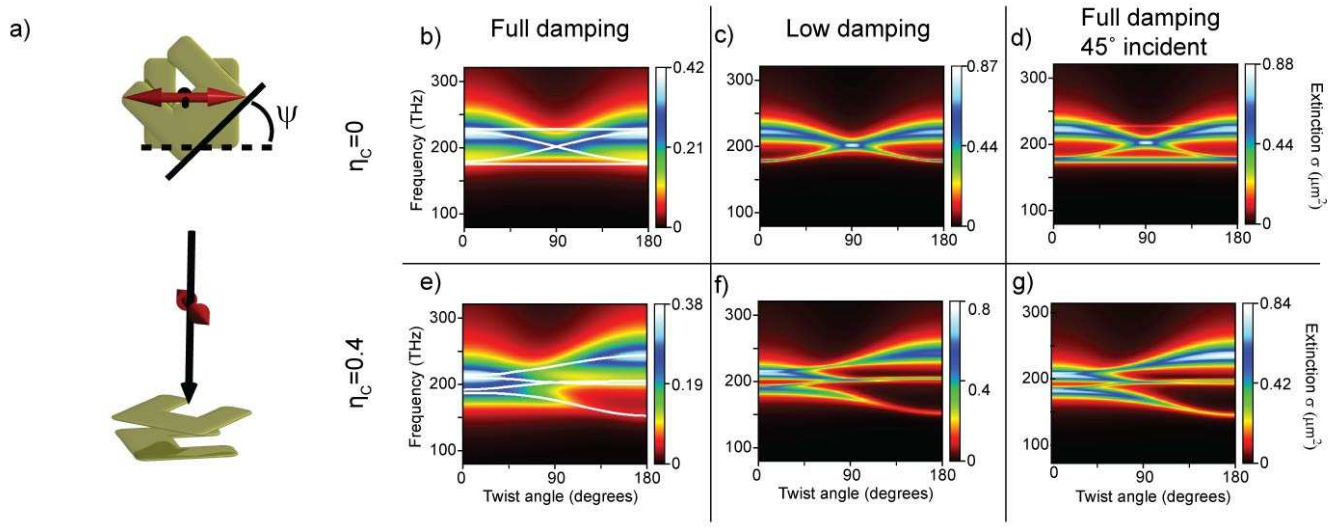

FIG. 3. Extinction cross sections σ_{ext} versus frequency and twist angle for an SRR stereodimer structure. Panel (a) shows the geometry (top view and side view) in which two SRRs are vertically stacked. The upper SRR is rotated around the z-axis by the twist angle ψ. We calculate extinction for light impinging from the z-direction with polarization along x, i.e., along the base of the lower SRR in (b,c,e,f). In (d,g) we use 45° incidence in the xz-plane, so that the H-field of the excitation light directly couples also to the magnetic polarizability. Panels (b), (c) and (d) show extinction assuming no cross coupling term ($\eta_C = 0$) while (e), (f) and (g) show extinction assuming strong magneto-electric coupling $\eta_C = 0.4$). Panels (b) and (e) assume the damping rate of gold $\gamma = 1.25 \times 10^{14}$ s^{-1}. To more clearly bring out the four mode structure, we reduce the damping ten-fold for the calculations in (c,d,f, g). There are four modes present in the system. White lines in (b,e) indicate the frequencies of the modes, as taken from the resonances in the low-damping case, i.e., the resonances in panels (d,g). Since

resonances in extinction. The blue shifted resonance is now observed to cross with a narrow red shifted resonance. The crossing is symmetric around 90° and is consistent with the hybridization of an electric dipole fixed along x, with a second one above it twisted by an amount ψ. The two branches have a very different width and strength, consistent with the fact that a symmetric configuration of dipoles couples more strongly to external fields (blue shifted resonance), than an antisymmetric 'dark' configuration (red shifted resonance).

To verify whether the two resonances observed in Fig. 3(a) are all resonances in the system, we change the angle of incidence to 45° in the xz plane, so that the exciting field has an H_z component to drive the split rings, in addition to an E_x component. Figure 3(d) shows that in this case four resonances occur in extinction. In addition to the two curved bands excited by E_x, there are also two non-dispersive bands with a twist independent splitting. Obviously, these bands are due to the coupling of two magnetic dipoles in symmetric (broad and intense band) and antisymmetric head-to-tail configuration. The existence of four instead of two modes is a new insight compared to LC circuit models[33,36], but is logical in view of the fact that split rings have both a magnetic and an electric response, which are decoupled under the assumption $\eta_C = 0$.

Next we analyze the extinction in presence of magneto-electric coupling, setting $\eta_C = 0.4$. Again, we first examine the extinction in presence of realistic loss ($\gamma = 1.25{\cdot}10^{14}\,\mathrm{s}^{-1}$) for gold in Fig. 3(e). As also predicted by FDTD simulations by Liu et al.[33], there appear to be two bands. The blue-shifted band is again very broad, but now has a frequency shift away from the single SRR resonance that is significantly larger for twist angle 180° than for 0°. These effects were explained by Liu et al. as due to an additive (subtractive) correction to the dominant electric hybridization at twist angle 180° (0°) that occurs due to magnetic dipole coupling. A surprise is that the diagram is not symmetric anymore around 90° twist as in the case of zero magnetic coupling. Instead, the extinction appears to show an anticrossing at twist angle 60° These features were also predicted by FDTD simulations by Liu et al.[33] However, the presence of an anticrossing at twist angle $\psi = 60^\circ$ could not be interpreted Liu et al [33] within an LC electrostatic circuit model, except by invoking higher order multipolar corrections. Here we see that a purely dipolar model may also explain all features of the experiment provided that magneto-electric coupling is accounted for. While we do not claim that multipolar effects are not present in actual experiments, it is an important insight that split ring polarizabilities with magneto-electric coupling terms may provide much richer physics then expected from electrostatic circuit theory. A main advantage of point dipole theory is that the underlying mode structure does not need to be recouped from FDTD simulations, but is easily resolved by repeating a calculation of extinction cross sections with low loss (as done in Fig. 3), or by analyzing the poles of the coupling matrix in Eq. (29) that relates $(\boldsymbol{p}, \boldsymbol{m})$ to $(\boldsymbol{E}_{\mathrm{in}}, \boldsymbol{H}_{\mathrm{in}})$. The computational effort for N split rings is equivalent to diagonalizing or inverting a $6N \times 6N$ matrix.

To more clearly bring out all the resonances we artificially reduce the damping $\gamma = 1.25 \cdot 10^{13}$ s^{-1} to ten times less than the damping of gold, and plot the response of the system under normal incidence (f) and 45° incidence (g) in Fig. 3 (f,g).

The anticrossing at twist angle $\psi = 60°$ appears to be due to the coupling of four modes, as opposed to the intuition from LC circuit theory that only two resonances anticross. The existence of four, rather than two modes in a split ring dimer appears surprising and is a second indication of the rich physics of magneto-electric scatterers. Intuition from LC circuits is that although the subspace of driving fields is two dimensional (E_x and H_z), nonetheless only one mode per split ring exists. The usual reasoning in LC models is that the relation between electric and magnetic dipole moment is completely fixed and independent of driving, since the loop current and accumulated charge are directly related. Such a constraint is not general: in electrodynamic multipole expansions, magnetic polarizabilties are determined independently from the electric ones. The intuition from LC theory that there is only one mode per scatterer is only retrieved in our model right at the limit of strongest magneto-electric coupling $\eta_C = \sqrt{\eta_E \eta_H}$, since in that case one polarizability is identically zero. We note that the values $\eta_E = 0.7, \eta_H = 0.3, \eta_C = 0.4$ used in this work (that we fitted to our angle-resolved transmission experiments on 200x200 nm Au split rings on glass) are close to the limit of strong magneto-electric coupling. Whether a general argument exists why physical scatterers are or are not exactly at the limit of strongest magneto-electric coupling $\eta_C = \sqrt{\eta_E \eta_H}$ is a question outside the scope of this paper.

VI. CONCLUSION

In conclusion, we have developed a new multiple scattering theory by means of which we can calculate scattering and extinction for any magneto-electric scatterer with known polarizability tensor, as well as for arbitrary finite clusters. As opposed to LC circuit models, our new model obeys energy conservation, contains all interference effects, and allows quantitative prediction of absolute cross sections, spectral linewidths and lineshapes. While outside the scope of this paper, the theory is readily extended to deal with arbitrary periodic lattices by generalizing Ewald lattice sums[41] to deal with both $\boldsymbol{E}$ and $\boldsymbol{H}$. Since the electrodynamic polarizability tensor can be directly constructed from electrostatic circuit theory, we expect that our model is readily applicable to many current experiments using chiral and nonchiral metamaterial building blocks for which electrostatic models have been proposed.

Our model does not give any insight into whether the response of a given structure is truly dipolar or not. Also, our model does not provide any insight or quantitative predictions based on microscopic considerations for the magnitude of the polarizability. For such microscopic considerations, based on, e.g., current density distributions derived from full wave simulations, we refer to [18–20,35,37,38]. Rather, our model allows one to verify if specific data or microscopic calculations are consistent at all with point dipole interactions, allowing to verify or falsify common intuitive explanations in literature that have sofar always been based on electrostatic considerations. Also, our model allows one to assess if a single polarizability tensor indeed can describe a range of different experiments with, e.g., split ring clusters, as should be expected from a consistent model. Finally, our model is the simplest electrodynamical model to consistently describe how metamaterials and photonic crystals are formed from magneto-electric scatterers. A first step is to confirm the parameters used in this work for η_E, η_H and η_C by targeted experiments. While the value for η_E used in this work is consistent with the extinction cross section measured by Husnik et al.[17], we propose that the new insight that magneto-electric coupling is far stronger than the magnetic polarizability be confirmed by off-normal circularly polarized extinction measurements as proposed in section IV.

The most important property of our theory is that a polarizability tensor validated for a single scatterer can readily be used to predict all quantitative scattering properties of composite lattices and antennas. We hence expect that new insights can be obtained in effective medium constants of metamaterial arrays. Our analytical model not only facilitates design, but will also for the first time allow to determine rigorously whether, even in the ideal case (no loss, no multipole corrections), metamaterial building blocks can give rise to a desired ϵ and μ, despite the large importance of electrodynamic corrections[7,9,60]. In addition to generating new insights for metamaterials, our theory also opens new design routes for gratings and antennas with unprecedented polarization properties. As an example, in this paper we analyzed the four mode anticrossing due to magneto-electric coupling in stereo-dimers. This analysis is easily extended to magneto-electric Yagi-Uda antennas, diffractive gratings of chiral building blocks, and magneto-inductive waveguides that may provide new ways to control the propagation and emission of light[46,61,62].

ACKNOWLEDGMENTS

We thank Ad Lagendijk for stimulating and inspirative insights, as well as Dries van Oosten and Lutz Langguth for discussions. This work is part of the research program of the "Stichting voor Fundamenteel Onderzoek der Materie (FOM)," which is financially supported by the "Nederlandse Organisatie voor Wetenschappelijk Onderzoek (NWO)."

Appendix A: Unit system

Throughout this paper we used units that significantly simplify notation throughout, as they maximimize the interchangeability of electric and magnetic fields. Conversion to SI units is summarized in Table I. For the conversion in Table I, we use ϵ for the host dielectric constant, c for the velocity of light, and Z for the impedance of the background medium. In this unit system, a plane wave has $|\boldsymbol{E}|/|\boldsymbol{H}| = 1$, and intensity $I = |\boldsymbol{E}|^2/(2Z)$, since the Poynting vector is $\boldsymbol{S} = 1/(2Z)\mathrm{Re}(\boldsymbol{E}^* \times \boldsymbol{H})$. In these units, the cycle-averaged work done by an electric field $\boldsymbol{E}$ to drive an oscillating $\boldsymbol{p}$ equals $W = 2\pi k/Z \mathrm{Im}(\boldsymbol{E} \cdot \boldsymbol{p})$. The magnetic counterpart is $W = 2\pi k/Z \mathrm{Im}(\boldsymbol{H} \cdot \boldsymbol{m})$

Quantity	Symbol	Relation to SI
Electric field	$\boldsymbol{E}$	$\boldsymbol{E}_{\mathrm{SI}}$
Magnetic field	$\boldsymbol{H}$	$Z\boldsymbol{H}_{\mathrm{SI}}$
Electric dipole moment	$\boldsymbol{p}$	$\boldsymbol{p}_{\mathrm{SI}}/(4\pi\epsilon)$
Magnetic dipole moment	$\boldsymbol{m}$	$\boldsymbol{m}_{\mathrm{SI}}(Z/(4\pi))$
Electric-electric polarizability	$\boldsymbol{\alpha}_{EE}$	$\boldsymbol{\alpha}_{EE}^{\mathrm{SI}}/(4\pi\epsilon)$
Magnetic-magnetic polarizability	$\boldsymbol{\alpha}_{HH}$	$\boldsymbol{\alpha}_{HH}^{\mathrm{SI}}/(4\pi)$
Electric-magnetic polarizability	$\boldsymbol{\alpha}_{EH}$	$\boldsymbol{\alpha}_{EH}^{\mathrm{SI}}(c/(4\pi))$
Magnetic-electric polarizability	$\boldsymbol{\alpha}_{HE}$	$\boldsymbol{\alpha}_{HE}^{\mathrm{SI}}(Z/(4\pi))$
Electric-electric Green tensor	$\boldsymbol{G}_{EE}$	$4\pi\epsilon\boldsymbol{G}_{EE}^{\mathrm{SI}}$
Magnetic-magnetic Green tensor	$\boldsymbol{G}_{HH}$	$4\pi\boldsymbol{G}_{EE}^{\mathrm{SI}}$
Electric-electric Green tensor	$\boldsymbol{G}_{EH}$	$4\pi/Z\,\boldsymbol{G}_{EE}^{\mathrm{SI}}$
Magnetic-magnetic Green tensor	$\boldsymbol{G}_{HE}$	$4\pi/c\,\boldsymbol{G}_{EE}^{\mathrm{SI}}$

TABLE I. Conversion between SI units and the unit system used throughout this paper.

* i.sersic@amolf.nl; http://www.amolf.nl/research/resonant-nanophotonics/
† Present address: Fritz-Haber-Institut der Max-Planck-Gesellschaft, Arnimallee 14, 14195 Berlin, Germany

[1] V. G. Veselago, Sov.Phys. USPEKHI **10**, 509-514 (1968).
[2] J. B. Pendry, Phys. Rev. Lett. **85**, 3966 (2000).
[3] J. B. Pendry, Physics World **14**, 47 (2001); C. M. Soukoulis, S. Linden, and M. Wegener, Science **315**, 47 (2007); V. M. Shalaev, Nature Photonics **1**, 41 (2007).
[4] U. Leonhardt, Science **312**,1777 (2006); J. B. Pendry, D. Schurig, and D. R. Smith, *ibid*, 1780 (2006).
[5] D. R. Smith, W. J. Padilla, D. C. Vier, S. C. Nemat-Nasser, and S. Schultz, Phys. Rev. Lett. **84**, 4184 (2000); W. J. Padilla, A. J. Taylor, C. Highstrete, M. Lee, and R. D. Averitt, *ibid.* **96**, 107401 (2006); S. Linden, C. Enkrich, M. Wegener, J. Zhou, T. Koschny, and C. M. Soukoulis, Science **306**, 1351 (2004).
[6] C. Enkrich, M. Wegener, S. Linden, S. Burger, L. Zschiedrich, F. Schmidt, J. F. Zhou, T. Koschny, and C. M. Soukoulis, Phys. Rev. Lett. **95**, 203901 (2005).
[7] C. Rockstuhl, T. Zentgraf, H. Guo, N. Liu, C. Etrich, I. Loa, K. Syassen, J. Kuhl, F. Lederer, and H. Giessen, Appl. Phys. B **84**, 219 (2006).
[8] M. W. Klein, C. Enkrich, M. Wegener, C. M. Soukoulis, and S. Linden, Opt. Lett. **31**, 1259 (2006).
[9] I. Sersic, M. Frimmer, E. Verhagen and A. F. Koenderink, Phys. Rev. Lett. **103**, 213902 (2009).
[10] B. Lahiri, S. G. McMeekin, A. Z. Khokhar, R. M. De La Rue, and N. P. Johnson, Opt. Expr. **18**, 3210 (2010).
[11] V. M. Shalaev, W. Cai, U. K. Chettiar, H.-K. Yuan, A. K. Sarychev, V. P. Drachev, and A. V. Kildishev, Opt. Lett. **30**, 3356 (2005).
[12] G. Dolling, C. Enkrich, M. Wegener, J. F. Zhou, C. M. Soukoulis, and S. Linden, Opt. Lett. **30**, 23 (2005).
[13] G. Dolling, C. Enkrich, M. Wegener, C. M. Soukoulis, and S. Linden, Opt. Lett. **31**, 12 (2006).
[14] G. Dolling, C. Enkrich, M. Wegener, C. M. Soukoulis, and S. Linden, Science **312**, 892 (2007)
[15] J. Valentine, S. Zhang, T. Zentgraf, E. Ulin-Avila, D. A. Genov, G. Bartal, and X. Zhang, Nature **455**, 376 (2008).
[16] S. P. Burgos, R. de Waele, A. Polman, and H. A. Atwater, Nature Mat. **9**, 407 (2010).
[17] M. Husnik, M. W. Klein, N. Feth, M. König, J. Niegemann, K. Busch, S. Linden and M. Wegener, Nature Photonics **2**, 614 (2008).
[18] C. Rockstuhl, F. Lederer, C. Etrich, T. Zentgraf, J. Kuhl, and H. Giessen, Opt. Expr. **14**, 8827 (2006).
[19] T. D. Corrigan, P. W. Kolb, A. B. Sushkov, H. D. Drew, D. C. Schmadel, and R. J. Phaneuf, Opt. Expr. **16**, 19850 (2008).
[20] A. Pors, M. Willatzen, O. Albrektsen, and S. I. Bozhevolnyi, J. Opt. Soc. Am. B **27**, 1680 (2010).
[21] E. Prodan, C. Radloff, N. J. Halas and P. Nordlander, Science **302**, 419 (2003).
[22] P. Banzer, U. Peschel, S. Quabis, and G. Leuchs, Opt. Expr. **18**, 10905 (2010).
[23] N. Feth, M. König, M. Husnik, K. Stannigel, J. Niegemann, K. Busch, M. Wegener, and S. Linden, Opt. Express **18**, 6545 (2010).
[24] M. Decker, S. Burger, S. Linden, and M. Wegener, Phys. Rev. B **80**, 193102 (2009).
[25] J. K. Gansel, M. Thiel, M. S. Rill, M. Decker, K. Bade, V. Saile, G. von Freymann, S. Linden, and M. Wegener, Science **325**, 1513 (2009).
[26] E. Plum, J. Zhou, J. Dong, V. A. Fedotov, T. Koschny, C. M. Soukoulis, and N. I. Zheludev, Phys. Rev. B **79**, 035407 (2009).
[27] E. Plum, X.-X. Liu, V. A. Fedotov, Y. Chen, D. P. Tsai, and N. I. Zheludev, Phys. Rev. Lett. **102**, 113902 (2009).
[28] S. Zhang, Y.-S. Park, J. Li, X. Lu, W. Zhang, and X. Zhang, Phys. Rev. Lett. **102**, 023901 (2009).
[29] B. Wang, J. Zhou, T. Koschny, M. Kafesaki, and C. M. Soukoulis, J. Opt. A: Pure Appl. Opt **11**, 114003 (2009).
[30] E. Plum, V. A. Fedotov and N. I. Zheludev, J. Opt. A: Pure Appl. Opt. **11**,074009:1-7 (2009).

[31] M. Decker, M. W. Klein, M. Wegener, S. Linden, Opt. Lett. **32**, 856 (2007).

[32] M. Decker, R. Zhao, C. M. Soukoulis, S. Linden, M. Wegener, Opt. Lett. **35**, 1593 (2010).

[33] N. Liu, H. Liu, S. Zhu and H. Giessen, Nature Photonics **3**, 157 (2009).

[34] H. Guo, N. Liu, L. Fu, T. P. Meyrath, T. Zentgraf, H. Schweizer, and H. Giessen, Opt. Expr. **15**, 12095 (2007).

[35] J. Petschulat, J. Yang, C. Menzel, C. Rockstuhl, A. Chipouline, P. Lalanne, A. Tennermann, F. Lederer, and T. Pertsch, Opt. Express **18**, 14454 (2010).

[36] H. Liu, J. X. Cao, S. N. Zhu, N. Liu, R. Ameling and H. Giessen, Phys. Rev. B **81**, 241403(R) (2010).

[37] C. Rockstuhl, T. Zentgraf, E. Pshenay-Severin, J. Petschulat, A. Chipouline, J. Kuhl, T. Pertsch, H. Giessen, and F. Lederer, Opt. Expr. **15**, 8871 (2007).

[38] J. Zhou, Th. Koschny, and C. M Soukoulis, Opt. Expr. **15**, 17881 (2007).

[39] A. Lagendijk and B. A. van Tiggelen, Phys. Rep. **270**, 143 (1996).

[40] P. de Vries, D. V. van Coevorden and A. Lagendijk, Rev. Mod. Phys. **70**, 2 (1998).

[41] F. J. García de Abajo, Rev. Mod. Phys. **79**, 1267 (2007).

[42] L. D. Landau and E. M. Lifshitz, *Electrodynamics of Continuous Media*, Pergamon, Oxford (1960).

[43] I. V. Lindell, A. H. Sihvola, S. A. Tretyakov, and A. J. Viitanen, *Electromagnetic Waves in Chiral and Bi-Isotropic Media*, Artech House, Norwood MA (1994).

[44] R. Merlin, Proc. Nat. Acad. Sci. **106**, 1693 (2009).

[45] W. H. Weber and G. W. Ford, Phys. Rev. B. **70**, 125429 (2004).

[46] A. F. Koenderink and A. Polman, Phys. Rev. B **74**, 033402 (2006). (2007).

[47] J. Garcìa-Garcìa, F. Martìn, J. D. Baena, R. Marqès and L. Jelinek, J. Appl. Phys. **98**, 033103 (2005).

[48] C. F. Bohren and D. R. Huffman, *Absorption and Scattering of Light by Small Particles*, John Wiley & Sons, New York (1983).

[49] N. Katsarakis, T. Koschny, M. Kafesaki, E. N. Economou, and C. M. Soukoulis, Appl. Phys. Lett. **84**, 2943 (2004).

[50] Note that the above equation should strictly be written with $\boldsymbol{\alpha}$ replaced by the t-matrix, which is directly proportional to the dynamic polarizability $\boldsymbol{\alpha}$ for point scatterers[39].

[51] J. D. Jackson, *Classical Electrodynamics (3rd ed.*, John Wiley & Sons, New York (1999).

[52] H. C. van de Hulst, *Light Scattering by Small Particles* (Dover, New York, 1981).

[53] M. Meier and A. Wokaun, Opt. Lett. **8**, 581 (1983); K. T. Carron, W. Fluhr, A. Wokaun and H. W. Lehmann, J. Opt. Soc Am. B **3**, 420 (1986); K. L. Kelly, E. Coronado, L. L. Zhao and G. C. Schatz, J. Phys. Chem. B **107**, 668 (2003); A. Wokaun, J. P. Gordon and P. F. Liao, Phys. Rev. Lett. **48**, 1574 (1982).

[54] M. Burresi, D. van Oosten, T. Kampfrath, H. Schoenmaker, R. Heideman, A. Leinse and L. Kuipers, Science **326**, 550 (2009); M. Burresi, T. Kampfrath, D. van Oosten, J. C. Prangsma, B. S. Song, S. Noda and L. Kuipers, Phys. Rev. Lett. **105**, 123901 (2010).

[55] M. G. Silveirinha,Phys. Rev. B **82**, 085101 (2010)

[56] R. Zhao, J. Zhou, Th. Koschny, E. N. Economou, and C. M. Soukoulis, Phys. Rev. Lett. **103**, 103602 (2009); M. G. Silveirinha and S. I. Maslovski, Phys. Rev. Lett. **105**, 189301 (2010); R. Zhao, J. Zhou, Th. Koschny, E. N. Economou, and C. M. Soukoulis, Phys. Rev. Lett. **105**, 189302 (2010).

[57] P. B. Johnson and R. W. Christy, Phys. Rev. B **6**, 4370 (1972).

[58] I. Sersic, A. Opheij and A. F. Koenderink, *in preparation.*

[59] Note that the diagonal elements of the electrodynamic polarizability do contain contributions due to off-diagonal elements in the electrostatic tensor. The radiation damping correction in Eq. (26) mixes η_C onto the diagonal.

[60] C. Menzel, T. Paul, C. Rockstuhl, T. Pertsch, S. Tretyakov, and F. Lederer, Phys. Rev. B **81**, 035320 (2010).

[61] A. F. Koenderink, Nano Lett. **9**, 4228 (2009).

[62] H. Liu, D. A. Genov, D. M. Wu, Y. M. Liu, J. M. Steele, C. Sun, S. N. Zhu, and X. Zhang, Phys. Rev. Lett. **97**, 243902 (2006).